Energy Reports 8 (2022) 11646–11660

Contents lists available at ScienceDirect

Energy Reports

journal homepage: www.elsevier.com/locate/egyr

Research paper

A novel AI approach for optimal deployment of EV fast charging station and reliability analysis with solar based DGs in distribution network

Fareed Ahmad [a], Imtiaz Ashraf [a], Atif Iqbal [b,*], Mousa Marzband [c,d], Irfan Khan [e]

[a] Department of Electrical Engineering, Aligarh Muslim University, Aligarh, India
[b] Department of Electrical Engineering, Qatar University, Doha, Qatar
[c] Department: Mathematics, Physics and Electrical Engineering, Northumbria University, UK
[d] Center of Research Excellence in Renewable Energy and Power Systems, King Abdulaziz University, Jeddah, 21589, Saudi Arabia
[e] Clean and Resilient Energy Systems (CARES) Lab, Texas A&M University, Galveston, TX 77573, USA

ARTICLE INFO

Article history:
Received 28 March 2022
Received in revised form 1 September 2022
Accepted 12 September 2022
Available online xxxx

Keywords:
Artificial Intelligence
Fast-charging stations
Bald eagle search algorithm
Optimal placement
Electric vehicle
Reliability

ABSTRACT

The transportation sector is one of the most prevalent fossil fuel users worldwide. Therefore, to mitigate the impacts of carbon-dioxide emissions and reduce the use of non-environmentally friendly traditional energy resources, the electrification of the transportation system, such as the development of electric vehicles (EV), has become crucial. For impeccable EVs deployment, a well-developed charging infrastructure is required. However, the optimal placement of fast charging stations (FCSs) is a critical concern. Therefore, this article provides a functional approach for identifying the optimal location of FCSs using the east delta network (EDN). In addition, the electrical distribution network's infrastructure is susceptible to changes in electrifying the transportation sector. Therefore, actual power loss, reactive power loss, and investment cost are three areas of consideration in deploying FCSs. Furthermore, including FCSs in the electricity distribution network increases the energy demand from the electrical grid. Therefore, this research paper recommends integrating solar-based distributed generations (SDGs) at selected locations in the distribution network, to mitigate the burden of FCSs on the system. Hence, making the system self-sustaining and reliable. In addition, the reliability of the distribution system is also analyzed after deploying the FCSs and SDGs. Furthermore, six case studies (CS) have been proposed to deploy FCSs with or without DG integration. Consequently, the active power loss went from 1014.48 kW to 829.68 kW for the CS-6.

1. Introduction

Incorporating distributed generations (DGs) and electric vehicle charging stations (EVCSs) into existing power networks has necessitated rapid changes within the system. This growing demand for solar based distributed generations (SDGs) due to its environmental benefits, the declining costs compared to traditional energy generation, technical advancement, and ease of use are major factors driving the SDGs market size (Reports, 2020). The increasing use of SDGs, wind power generation, and other DGs technologies have paved the way for small and medium scale involvements, thus, resulting in the coining of the word prosumers, which refers to people who deliver and consume energy at the same time (Lotfi et al., 2019). SDG has not only been shown to be environmentally friendly, but it has also been proven to decentralize the electrical power network, lowering power losses and enhancing bus voltages (Sambaiah and Jayabarathi, 2021).

These distributed renewable energy technologies could help minimize reliance on fossil fuels as they aid the rapid growth of EVs and reduce greenhouse gas (GHG) emissions in the transportation system (Luo et al., 2020; Bilal and Rizwan, 2021). Moreover, with the emergence of EVs, there is a growing global concern about the continual use of petroleum-based products in the transportation sector due to their environmental impacts and depletion (Gandoman et al., 2019). Furthermore, EVs have advantages such reduced noise pollution, lower operational costs, and emission-free (Michaelides, 2021; Ahmad et al., 2022a).

The rapid adoption of EVs is strongly reliant on the quick growth of charging infrastructure. The EV chargers have three charging levels based on charging time and power level; Level 1 (slow), Level 2 (medium), and Level 3 (fast), and they can be onboard or offboard. Level 1 and level 2 chargers are onboard charging, whereas level 3 charger is offboard. However, level 1 and level 2 chargers are limited by power density and charging time, while level 3 chargers are the fastest (Luo et al., 2017). In

* Corresponding author.
E-mail address: atif.iqbal@qu.edu.qa (A. Iqbal).

https://doi.org/10.1016/j.egyr.2022.09.058
2352-4847/

addition, EVs are predicted to minimize CO2 emissions by 50 to 100 g per kilometre (Nanaki and Koroneos, 2016; Ahmad et al., 2022c). In recent years, the EV industry in the United States has experienced significant growth, with EV sales rising from 16,000 vehicles in 2011 to over 2 million vehicles in 2021 (Electrek, 2021). As EVs become more popular in the United States, the need for EV charging stations is rapidly increasing.

This widespread of EVs in the transport industry will not only enhance the environment but will also optimize network stability by enabling frequency and voltage control while serving as the vehicle to grid (V2G) to mitigate for abrupt load rise or loss in the grid (Faddel et al., 2018). In contrast, the incorporation of EVCSs into the distribution network must be accomplished strategically because it may result in excessive loading, leading to higher power loss, power quality deterioration (Ahmed et al., 2021) and voltage deviations exceeding permitted thresholds (Deb et al., 2018). The problem worsens when more EVCSs is integrated into the distribution network, with widespread penetration of randomly distributed SDG. As a result, the appropriate placement of EVCSs in the distribution network is required to reduce their detrimental effects on the distribution network.

1.1. Related works

The cost of active and reactive power losses and the development of CS are set as objectives for finding the optimal location of CS, and the proposed problem have addressed using balanced mayfly techniques (Chen et al., 2021). In Mainul Islam et al. (2018), the authors devised a multi-objective optimization problem for the placement of FCSs using conveyance energy loss, installation cost and sub-station energy loss cost as objectives which have been addressed using the binary lighting search algorithm. In addition, Pal et al. (2021) presented an optimization problem incorporating energy loss, voltage variation, EV fleet and land cost as objective functions. However, the uncertainty related to the EVs has efficiently been controlled by the 2 m point estimation method (2 m PEM) and the optimal result was acquired by the Harris hawks optimization technique.

Furthermore, the station investment cost, specific energy consumption cost of the EVs, network power loss and voltage deviation are suggested for the optimization problem. Therefore, a novel hybrid shuffled frog leap-teaching learning-based optimization (SFL-TLBO) technique was utilized to address the problem (Battapothula et al., 2019). The literature provides power loss, voltage shape and EV charging costs as objective functions for the problem formulation of finding the optimal placement of the CSs and RESs (Moradi et al., 2015). Furthermore, in Bitencourt et al. (2021), the bat algorithm is employed to solve the objective function for the placement of CS, which is the minimization of electrical power loss and charging zone center. Moreover, in Cheng et al. (2022) the authors optimized the location and size of the EV charging station considering traffic information and area division and proposed problem obtained by the improved whale optimization algorithm. In Li et al. (2022), used charging costs, total investment costs, and operating costs of the charging stations are formulated as the objective functions for the proposed problem to deploy the charging station integration of renewable energy and energy storage.

In Reddy and Selvajyothi (2020), a power loss of an imbalanced radial distribution network was offered as an objective for EVCS deployment, and the described optimization problem was handled using the particle search optimization algorithm. Furthermore, Mohsenzadeh et al. (2018) explored the optimal placement of parking lots by increasing parking lot earnings and used the cost of power loss, reliability, voltage deviation, and parking lot as the objectives with the genetic algorithm (GA) delivering the optimal findings. A similar topic is addressed in Ahmad et al. (2022b), which takes into account installation costs and active power loss costs for placement, as well as an optimization problem responded by the gray wolf optimization algorithm. For (Luo and Qiu, 2020), the concentration was on the optimal deployment of the CS for sustainable cities, and they suggested a multi-objective problem. Also, the annualized time opportunity cost, travel cost, construction cost and operation cost are supposed objective functions and GA addressed the offered problem. Furthermore, in Rajesh and Shajin (2021) found the optimal location of CSs and capacitors while accounting for power loss costs and the defined issue is addressed using the Quantum-Behaved and Gaussian Mutational Dragonfly Algorithm.

The reliability of the distribution system has been analyzed after the placement of the charging station and DGs in Bilal et al. (2021). In contrast, the power loss and voltage deviation cost are used as objective functions and proposed problem solved by hybrid gray wolf optimization particle swarm optimization algorithm. In addition, the reliability indices, power loss, voltage deviation are used for the placement of the charging station in which a meta-heuristic algorithm addresses the proposed problem in Matlab/Simulink (Archana and Rajeev, 2021).

1.2. Findings and contributions

A significant number of researchers have explored the installation of charging stations without considering the integration of renewable distributed generation, which is not so viable in the large-scale deployment of EVs. The integration of charging station to the grid is not beneficial for the environment because the grid power generation mostly from the conventional sources. Furthermore, all the article which place the charging stations at optimal locations, is not analyzed the reliability of the system. Therefore, the objective of this research to place the charging station at optimal location with renewable energy generation and also have analyzed the reliability indices of the distribution system for different case studies.

To investigate the impact on system reliability, fundamental system reliability indicators such as the system average interruption frequency index (SAIFI), system average interruption duration index (SAIDI), Customer Average Interruption Duration Index (CAIDI), and expected energy not supplied (EENS) and average energy not supplied (AENS), among others, are used. This research introduces a novel improved bald eagle search algorithm for placing FCSs in a distribution network with SDG. The SDG generation are placed and distributed randomly on the load nodes of the EDN distribution network, which serves as the case study network. The neoteric contributions of this paper are:

1. An improved BES for optimizing the placement of FCSs in the distribution network. To the authors' knowledge, an IBES has never been employed for charging station location.
2. Considering a distribution network with SDG that are randomly sized and located to represent real-life consumer-based decentralized penetration. Most studies include dispersed generations to adjust for the effects of the FCSs on the distribution network. On the other hand, this study includes the FCSs and distributed SDG across the distribution network.
3. The optimal location of the fast-charging station is modeled using three objectives. The operational parameters of the distribution network are taken into account by imposing a penalty for exceeding the safe limit. Hence, the complex optimal location problem is modeled as a optimization problem while taking into account the operating parameters of the system, which may adversely undermine the safety of the system.
4. The customer oriented and energy oriented reliability indices of the distribution system is also explored before and after the deployment of FCSs for different case studies.

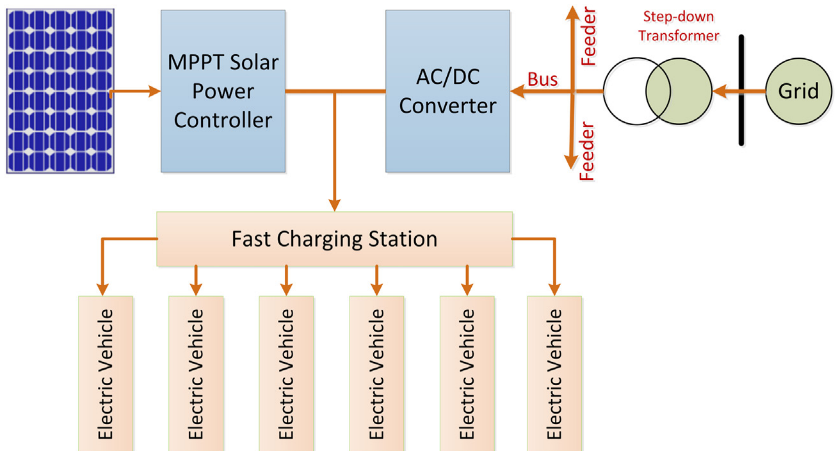

Fig. 1. Single line diagram of the charging station.

2. Problem formulation

One of the main focus of this research is identifying the optimal location for the FCSs. This is a multi-objectives problem with various economic factors such as operation and maintenance costs, station equipment costs, and land costs. Therefore, specific cost function indices are introduced to handle the deteriorating performance of the distribution system for the placement of FCSs. Furthermore, the research identifies the number of FCS in the suggested region before evaluating their optimal location. The single line block diagram are presented in Fig. 1.

2.1. Placement and size of renewable energy sources

The integration of EV load into the grid is not beneficial, as discussed above, for reducing carbon emission if the power is generated from fossil fuels. Therefore, the addition of SDG into the grid is highly recommended. In addition, distributed location of the SDG is more reasonable for the system to reduce losses, reliability of system and voltage stability. Moreover, in this work, some locations are identified for the placement of SDGs, which have enough space and good atmospheric conditions for SDGs. Solar and wind energy technologies are two of the fastest growing renewable energy sources for distributed generation (Gielen et al., 2019). However, the integration of FCSs into the grid could mismatch power demand and electricity generation. This mismatch is resolved by including SDGs into the distribution network, which reduces the grid stress caused by EV load (Tavakoli et al., 2020). In addition, the power generated from the SDGs is assumed at 10% of the total load of the east delta network (EDN) (El-Ela et al., 2016), with a power factor of 0.95. Therefore, the total active and reactive power generated by the SDGs are estimated at 2520 kW and 828 kVAR respectively.

2.2. Number of fast charging station

The required number of FCSs in the selected case study region was calculated using the overall EV population in the area, the battery capacity, load factor and charging time. The derived equation is expressed in Eq. (1) (Phonrattanasak and Leeprechanon, 2012). Equally, the number of FCS (N_{FCS}) is shown.

$$N_{FCS} = \frac{p^{EV} \times N^{EV} \times Ch_{time}}{S_t \times Ef \times C_P \times lf \times N^C \times pf} \tag{1}$$

where, p^{EV} is the mean power of EVs, N^{EV} is the number of EVs to be charged per day, Ch_{time} is the charging time, S_t is the charger service time, C_p is the capacity of connector, N^C is the number of connectors in FCS, Ef is charging efficiency, lf is the load factor of the charger, and pf is the power factor of charging load.

2.3. Investment cost reduction indicator

The variation in land cost is dependent on the location examined. In addition, the development cost contributes significantly to the project's total cost. However, this cost will decline as technology improves in the future. Therefore, FCS investors need to investigate the land cost of each chosen location of the FCS. Then, the investment cost (IC) is calculated using the fixed cost, land cost and development cost of the connector, as indicated in Eq. (2). The planned FCS requires a minimum space of 100 m^2. Thus, the land cost is calculated as the land rental cost over five years. Furthermore, the normalized value of investment cost is expressed by the investment cost reduction indicator (ICRI) at ith bus, which is given in Eq. (3).

$$IC_i = C^{fix} + 100 \times N_D \times C_i^{lan} + (N_c - 1) \times C_p \times C_{dev} \tag{2}$$

$$ICRI_i = \frac{IC_i}{max(IC_i)} \tag{3}$$

where, C^{fix} is the fixed cost for establishing the charger, C_i^{lan} is the land rental cost per m^2 per day for five years at ith bus, which is developed erratically, C_p and N_c are the rated power of the connector and number of connector respectively, C_{dev} is the development cost of each connector, N_D is the number of days for suggested planning.

2.4. Active power loss reduction indicator

Two power loss reduction indicators were used to the examined EDN bus distribution system in determining the appropriate position of FCSs. The first power loss reduction indicator is the active power loss reduction indicator (PLRI). The PLRI evaluates possible increase in the grid power losses when the FCSs are connected. This is expressed in Eq. (4).

$$PLRI = 1 - \frac{PL^{Base}}{PL^{FCS}} \tag{4}$$

where, PL^{Base} and PL^{FCS} are the total active power loss of the distribution system without FCS placement and with FCS placement respectively. Furthermore, the active power loss of the system is determined by using Eq. (5).

$$PL = \sum_{b=1}^{Nb} \left(\frac{P_b^2 + Q_b^2}{V_b^2} \right) R_b \tag{5}$$

where, P_b, Q_b are the active and reactive power flow in bth branch of the network, respectively, R_b is the resistance of the bth branch whereas, V_b is the sending node voltage of the given branch and Nb is the total number of branches in given network.

2.5. Reactive power loss reduction indicator

The second power loss reduction indicator considered the reactive power loss reduction indicator (QLRI), which provides a specified threshold for maintaining the grid voltage stability when reactive power losses are less than it. This indicator is expressed in Eq. (6).

$$QLRI = 1 - \frac{QL^{Base}}{QL^{FCS}} \tag{6}$$

where, QL^{Base} and QL^{FCS} are the total reactive power loss of the distribution system without FCS placement and with FCS placement respectively. Furthermore, the reactive power loss of the system is calculated by using Eq. (7).

$$QL = \sum_{b=1}^{Nb} \left(\frac{P_b^2 + Q_b^2}{V_b^2} \right) X_b \tag{7}$$

where, P_b, Q_b are the active and reactive power flow in bth branch of the network, respectively, X_b is the reactance of the bth branch whereas, V_b is the sending node voltage of the given branch and Nb is the total number of branches in given network.

2.6. Reliability

The significant surge in load demand caused by EV fast-charging causes interruptions in the distribution network. The rise in load demand caused by unplanned charging affects reliability indices, especially the system reliability index (SRI), resulting in consumer discontent. SRIs are classified into two types: customer-oriented reliability indexes and energy-oriented reliability indexes. SAIFI, SAIDI and CAIDI are included in customer-oriented reliability indexes whereas EENS and AENS are considered in energy-oriented reliability indexes (Bilal et al., 2021). All the data which is required for the reliability analysis are borrowed (Archana and Rajeev, 2021; Bilal et al., 2021) for the proposed distribution network.

The reliability indices are laboriously influenced by statistical parameters such as failure rate and outage duration. Therefore, these parameters can be changed after integrating EV load and SDG generations. Furthermore, the rate for failure and duration of interruption for the given bus can be stated in Eqs. (8), (9)

$$\delta_{EV} = (P_{base} + \Delta P_{EV}) \frac{\delta_{base}}{P_{base}} \tag{8}$$

$$T_{EV} = (P_{base} + \Delta P_{EV}) \frac{T_{base}}{P_{base}} \tag{9}$$

where, P_{base}, δ_{base} and T_{base} are the base value of active power demand, failure rate and duration of outage for the distribution network. ΔP_{EV} is the active power load which is integrated due to EV for the distribution system.

Customer-oriented reliability indices include SAIFI, SAIDI, and CAIDI, whereas energy-oriented reliability indexes include EENS and AENS. SAIFI is calculated based on the number of disruptions experienced by the consumer during a given period. SAIFI degrades as the number of disruptions and customers in the system expansions, which is expressed as in Eq. (10).

$$SAIFI = \frac{\sum(\delta_{EV} \times C_i)}{\sum(C_i)} \tag{10}$$

where, C_i is the number of customers connected to ith bus after integration of FCSs and SDGs. SAIDI is determined by each client's total time of interruption for a particular instant with EV charging loads. It reflects the network's condition in terms of the extent of the interruption, as in Eq. (11)

$$SAIDI = \frac{\sum(T_{EV} \times C_i)}{\sum(C_i)} \tag{11}$$

CAIDI is calculated using the average failure rate, the time it takes for the failure rate to increase due to higher EV load, and the customer count. It denotes the average time it takes that a particular client must meet, as shown in (12)

$$CAIDI = \frac{\sum(T_{EV} \times C_i)}{\sum \delta_{EV} \times (C_i)} \tag{12}$$

As demonstrated in Eq. (13), the network's Expected Energy Not Supplied (EENS) is the product of load and interruption time. The EENS is a sign of insufficient energy.

$$EENS = \sum(P_{EV} \times T_i) \tag{13}$$

where, P_{EV} is the load of the distribution network after integration of EV. AENS is the measure that reveals the load demanded at the bus and provides knowledge on the cut of energy that is not available within a given time stand with the growth of additional charging loads. AENS is expressed in Eq. (14).

$$AENS = \frac{\sum(P_{EV} \times T_i)}{\sum(C_i)} \tag{14}$$

3. Cost function

The distribution system indicators discussed above and the FCS's acquisition cost are considered for analyzing the location of the CSs. The illustrated optimization problem is a mixed-integer nonlinear problem in which X_i is a binary variable. Hence, the cost function must be decreased to minimize the active and reactive power loss, and investment cost for the optimal placement of the FCS. The suggested objectives are formulated as a single objective optimization problem, which is expressed in Eq. (15).

$$f = w_1 \times PLRI + w_2 \times QLRI + w_3 \times \sum_{i=1}^{N} (ICRI_i \times X_i)/N_{FCS} \tag{15}$$

where, N is the buses in the distribution network, which are the possible location of FCS, X_i is the binary variable (0 or 1). *If $X_i = 0$, it indicates that no FCS is placed at the given bus, and if $X_i = 0$, it indicates that FCS must be placed at that bus.* where, w_1, w_2 and w_3 must follow the equality and inequality condition, which are expressed in Eqs. (16) and (17), respectively.

$$w_1 + w_2 + w_3 = 1 \tag{16}$$

$$0 \leqslant w_1, w_2, w_3 \leqslant 1 \tag{17}$$

w_1, w_2 and w_3 are the coefficients used to change the priorities in decision making between power loss of the distribution system and the investment cost of the FCS.

3.1. Constraints

For the optimal site of the charging stations, the expressed cost function must adhere to some inequality and equality restrictions.

Voltage limit constraint: The voltage at respective buses must follow a minimum and maximum boundary, which is defined in Eq. (18).

$$V^{min} \leqslant V_i \leqslant V^{max} \tag{18}$$

where i = 1, 2…N, V^{min} and V^{max} are the minimum and maximum voltage limits of respective buses, V_i is the voltage of ith bus, 0.90 and 1.10 are the defined minimum and maximum bus voltage value in per unit.

Active power limit constraints: In Eq. (19), an active power limitation is generated by maintaining the active power of each line under set constraints.

$$P^{min} \leqslant P_j \leqslant P^{max} \tag{19}$$

Table 1
Placements and size of SDGs for the EDN.

Distributed SDGs	Real power (kW)	Reactive power (kVAR)	Bus
SDG-1	840	276	5
SDG-2	1120	368	16
SDG-3	560	184	22

where j = 1, 2 …L, P^{min} is the minimum active power limit of the lines, P^{max} is the maximum active power limits of the lines, and P_j is the active power at jth line.

Reactive power limit constraints: To keep the reactive power of each line within set limits, a reactive power constraint is formed in Eq. (20).

$$Q^{min} \leqslant Q_j \leqslant Q^{max} \tag{20}$$

where j = 1, 2 …L, Q^{min} is the minimum reactive power, Q^{max} is the maximum reactive power of the lines, and Q_j is the reactive power at jth line.

Power balanced constraints: the power demand and generation should be equal, which is formulated in (21).

$$P_{EV} + P_{sys} = P_{PV} + P_{grid} \tag{21}$$

where, P_{sys} is the power demand of IEEE-34 bus system without EV integration, P_{grid} is the power consumption from the grid, P_{EV} is the EV power demand whereas P_{PV} is the power generated from the renewable energy sources.

Number of fast charging station: The number of fast charging is calculated using (22), therefore minimum restriction is applied for the number of FCS to minimized the cost function.

$$N_{FCS}^{min} \leqslant N_{FCS} \tag{22}$$

where N_{FCS}^{min} is the minimum number of fast-charging stations that should be placed in the proposed area; each charging station has a fixed number of connectors with 100 kVA as proposed.

4. Solution technique

Classical optimization techniques could find the optimal solution for the unconstrained maxima and minima continuous and differential functions. However, classical approaches have confined practical use, as they need objectives that are not continuous or differential. Hence, advanced optimization techniques are employed to accomplish the best solution for the specified problem.

4.1. An improved bald eagle search algorithm

The improved bald eagle search (IBES) algorithm (Ramadan et al., 2021) established on the bald eagle search algorithm (Alsattar et al., 2020), and it is motivated by bald eagle behavior during the hunting process. The hunting strategy involves selecting the space, searching the space, and swooping in on the prey.

Selecting the space: Using Eq. (23), the bald randomly selects the space by applying the previously searched information.

$$p_{new,i} = p_{best} + \alpha \times r(p_{mean} - p_i) \tag{23}$$

Instead of using a fixed value as required in the original BES method, a new parameter, alpha is used to manage the changes in position and can be derived using Eq. (24).

$$\alpha = \frac{(1.5 \times (Max_{Iter} - t + 1))}{(Max_{Iter})} \tag{24}$$

This new parameter affects the bald position of eagles and improves the exploration and exploitation of the IBES approach. r is a number between 0 and 1. The new and best search spaces are denoted by p_{new} and p_{best} respectively. p_{mean} shows the eagles have ingested all the details from the prior search.

Search stage: The eagles move in a spiral form to speed up prey search in the selected space. At this point, the eagle's location is updated using Eqs. (25), (26)–(29).

$$p_{i,new} = p_i + y(i) \times (p_i - p_{i+1})p_{best} + x(i) \times r(p_i - p_{mean}) \tag{25}$$

$$x(i) = \frac{xr(i)}{max|xr|}, y(i) = \frac{yr(i)}{max|yr|} \tag{26}$$

$$xr(i) = r(i) \times sin(\delta(i)), yr(i) = r(i) \times cos(\delta(i)) \tag{27}$$

$$\delta(i) = \alpha \times \pi \times rand \tag{28}$$

$$r(i) = \delta(i) \times R \times rand \tag{29}$$

where, α is a parameter with a range of 5 to 10, and R is a parameter with a range of 0.5 to 2.

Swooping stage: At this stage, the eagles begin to swing from an optimal search position towards their prey, as expressed in Eqs. (30)–(33).

$$p_{i,new} = rand \times p_{best} + x_1(i)(p_i - c_1 \times p_{mean}) + y_1(i)(p_i - c_2 \times p_{best}) \tag{30}$$

$$x_1(i) = \frac{xr(i)}{max|xr|}, y_1(i) = \frac{yr(i)}{max|yr|} \tag{31}$$

$$xr(i) = r(i) \times sinh(\delta(i)), yr(i) = r(i) \times cosh(\delta(i)) \tag{32}$$

$$\delta(i) = \alpha \times \pi \times rand, r(i) = \delta(i) \tag{33}$$

where, c_1 and c_2 have value from 1 to 2.

5. Results and discussions

This work was implemented using, MATLAB 2018a programming language, which was installed in a windows 8.1 computer with Intel i7 processor, 2.4 GHz clock speed and 4 GB RAM. The proposed multi-stage method was applied on East Delta Network (EDN) distribution systems to solve the optimal FCS placement problem. The EDN distribution system is a part of the Unified Egyptian Network (UEN) (El-Ela et al., 2016). Hence, the single line diagram of EDN is shown in Fig. 2. The line voltage, rated capacity and power factor are 11 kV, 27.221 MVA and 0.854 respectively. The location and sizing of the renewable distributed generation are presented in Table 1. Furthermore, the number of fast charging stations is derived using Eq. (1). The proposed FCS has 10 connectors, each connector is rated 100 kVA with 0.95 power factor.

5.1. Validation of improved bald eagle search algorithm

The IBES was tested and assessed against a variety of benchmark functions. The proposed IBES algorithm flowchart is presented in Fig. 3. In addition, the results from the IBES algorithm were compared with some other modern optimization techniques (AEO, GBO, BES) in Ramadan et al. (2021). Also, the results of the IGOA and GOA were compared with the proposed algorithm, and the parameters of related algorithm are provided in Table 2. Similarly, the results of the unimodal benchmark functions (F1–F7) and the multimodal benchmark functions (F8–F13) are illustrated in Table 3. Therefore, The IBES algorithm was proven to outperform other meta heuristic algorithms for the benchmark functions.

Table 2
Used parameters.

Parameters	Value	Unit
Population size (nPop.)	100	–
Max. Iterations (Max_{iter})	100	–
Number of runs (N^{runs})	30	–
Parameter of GBO	Pr = 0.5	–
Parameters of BES	c_1, c_2, α = 2, a = 10, R = 1.5	–
Parameters of IBES	c_1, c_2 = 2, a = 10, R = 1.5	–
Number of EVs (N^{EV})	2000	–
Charging time (Ch_{time})	0.33	h
Number of connector in FCS (N^C)	10	–
Service time of FCS (st)	18	h
Fixed cost of FCS (C_{fix})	21 900	$
Development cost of connector (C_{dev})	109.5	$
Charger efficiency (Ef)	0.9	–
Power factor of FCS (pf)	0.95	–
Load factor of FCS (lf)	0.9	–
Average power for each EV (p^{EV})	96	kW
Connector capacity (C_p)	100	kVA
Electricity price (C_E)	0.11	$/kWh
Number of days (N_D)	1825	–

Table 3
Results of benchmark functions (Ramadan et al., 2021).

Functions		IGOA	GOA	AEO	GBO	BES	IBES
F1	Best	8.36E−16	0.0683	7.97E−42	1.00E−23	0	0
	Worst	9.59E−15	4.4591	2.26E−33	9.21E−21	0	0
	Mean	3.34E−15	0.8386	2.50E−34	1.92E−21	0	0
F2	Best	9.06E−09	0.029	1.36E−22	4.32E−13	0	0
	Worst	6.59E−08	79.104	6.59E−17	1.03E−10	1.37E−270	4.47E−303
	Mean	2.44E−08	10.244	9.84E−18	1.96E−11	6.85E−272	2.73E−304
F3	Best	8.44E−12	450.45	3.44E−38	5.08E−50	0	0
	Worst	0.0983	4603.90	2.20E−30	7.79E−45	0	0
	Mean	0.0121	1789.34	2.84E−31	4.20E−46	0	0
F4	Best	9.7112E−08	3.0335	2.55E−21	3.69E−11	0	0
	Worst	0.0694	19.5647	8.30E−17	5.29E−10	1.51E−260	1.60E−294
	Mean	0.0257	9.7756	1.38E−17	2.49E−10	7.56E−262	8.32E−296
F5	Best	25.850	25.698	26.413	26.2035	23.423	23.491
	Worst	27.036	7522.99	27.87792	28.7239	25.7669	25.3265
	Mean	26.448	965.65	27.1144	27.289	24.2684	24.6636
F6	Best	5.2803E−07	0.0203	0.090625	0.03963	6.70E−7	1.43E−5
	Worst	2.52103−06	11.0963	0.66915	0.228144	7.96E−5	0.249381
	Mean	1.4451E−06	0.8997	0.333799	0.102408	1.79E−5	0.03938
F7	Best	1.0746E−05	0.0090	9.34E−5	0.000839	1.58E−5	2.25E−6
	Worst	0.0072	0.0602	0.009584	0.009435	0.000348	3.10E−4
	Mean	0.0010	0.0234	0.001969	0.002914	0.000142	8.49E−5
F8	Best	−9009.31	−8903.05	−1759.19	−1830.71	−1777.18	−1731.16
	Worst	−5993.93	−6468.56	−1400.39	−1642.02	−1043.35	−1354.55
	Mean	−7594.16	−7728.43	−1608.48	−1720.61	−1503.62	−1543.11
F9	Best	0	1.9899	0	0	0	0
	Worst	0	27.8586	0	0	0	0
	Mean	0	9.4853	0	0	0	0
F10	Best	8.58E−09	1.5021	8.88E−16	8.88E−16	8.88E−16	8.88E−16
	Worst	1.97E−08	4.5855	4.44E−15	3.70E−08	20	20
	Mean	1.30E−08	3.0892	1.24E−15	4.09E−09	18	11
F11	Best	6.66E−16	0.3226	0	0	0	0
	Worst	6 2.52E−14	1.0411	0	2.04E−09	0	0
	Mean	5.50E−15	0.6966	0	1.02E−10	0	0
F12	Best	4.62E−08	1.8994	0.001042	0.000366	2.91E−09	6.53E−06
	Worst	1.85E−07	9.7664	0.004707	0.002090	3.41E−07	9.95E−05
	Mean	8.93E−08	5.6658	0.002850	0.001236	1.04E−07	4.13E−05
F13	Best	4.85E−07	0.3005	0.530081	0.104263	2.247450	1.959950
	Worst	0.0989	35.2838	2.970408	0.475712	2.966102	2.968414
	Mean	0.0138	8.7624	1.665532	0.218800	2.904654	2.916155

5.2. Results of optimal location of FCS with SDG

In this study, the EDN 30 bus distribution system was used to illustrate the efficacy of the suggested improved BES algorithm. In addition, the neoteric IBES algorithm was used to assess the fitness value given in the objective function Eq. (15) against the varying w_1, w_2, and w_3 for the FCSs placement in the network. Therefore, this method provides optimal locations for FCSs with randomly positioned SDGs and minimizes the investment cost, real power loss and reactive power loss. The optimal number of

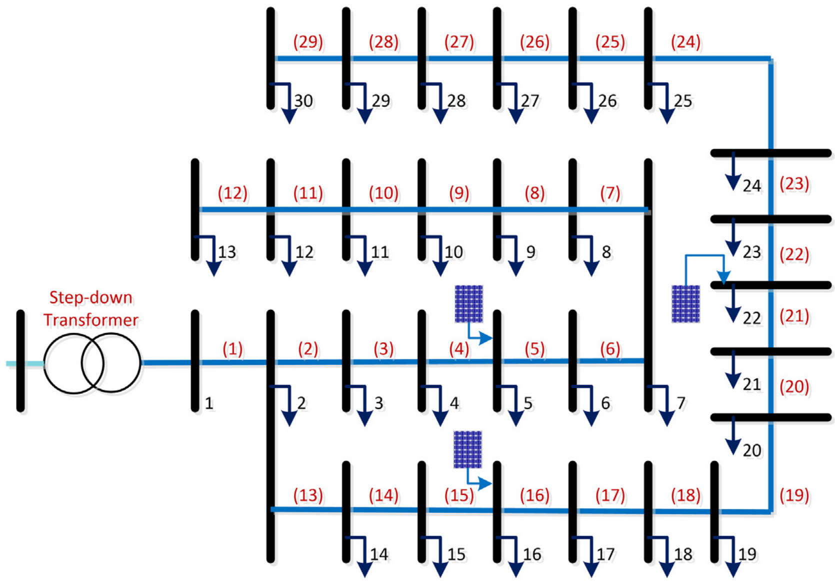

Fig. 2. Single line diagram of the EDN (Ahmad et al., 2022a).

FCSs required was five. However, 6 cases were offered for the placement of FCSs by modifying the values of w_1, w_2, and w_3. Moreover, to addressed the sensitivity analysis for optimization results of charging station location by varying the weight coefficient, six case studies were proposed to place the FCSs with renewable based distributed generations.

5.2.1. Results of optimal location of FCSs

For first case study (**CS1**), the active and reactive power losses are not considered for the optimization problem while the only investment cost is incorporated. However, in case study 2 (**CS2**), the optimal locations are obtained by incorporating 10% of active, 10% of reactive power loss while 80% of investment cost for optimization problem. The optimal location of FCSs obtained, in this case, is the same as the previous case due to the low value of power losses considered. Furthermore, in case study 3 (**CS3**), 20%, 20% and 60% of real power loss, reactive power loss and investment cost were considered. In case study 4 (**CS4**), active and reactive power losses are increased from 20% to 30% while the investment cost is reduced from 60% to 40%, hence, power losses are the dominating factors in the optimal location of the FCS. Similarly, in case study 5 (**CS5**), power loss inclusion is raised further and the investment cost is reduced in deciding the optimal location of the FCS. Finally, in the case study 6 (**CS6**), only power losses are considered for the placement of FCS, therefore, the optimal location of FCSs obtained in this case has less power losses compared with others proposed cases. The power losses obtained from **CS1** to **CS6** are continuously decreasing due to the increasing power losses in the objective function. The results obtained for the FCSs locations with real power losses, reactive power losses and cost function values for respective cases are given in Table 4. In addition, the real and reactive power flow for the lines in the EDN are obtained for all proposed cases. The derived real power flow decreases from for **CS1** to **CS6** as shown in Fig. 4. Similarly, the reactive power flow decreases from **CS1** to **CS6** in Fig. 5.

5.2.2. Results of optimal location of FCSs with SDGs

For **CS1**, the active and reactive power losses are not incorporating for the deciding factors of FCS deployment. Therefore, the higher power losses are obtained while comparing with other cases as shown in Table 4. Furthermore, in **CS2**, the optimal position of FCSs is determined by considering 10% of real power loss. In this case, the decision function accounts for 10% of reactive power loss and 80% of the investment cost, and due to negligible power losses, the optimal position of FCSs is the same. Furthermore, in **CS3**, 20%, 20%, and 60% of the true power loss, reactive power loss, and investment cost were taken into account in deciding the placement of the FCS. In **CS4**, power loss concerns are raised from 20% to 30%, while investment cost is lowered from 60% to 40%, resulting in power losses being the prevailing factor in the optimal location of FCS. Similarly, in **CS5**, the power loss inclusion is raised while the investment cost component is lowered in determining the optimal location of the FCS. However, in **CS6**, only power losses are considered in the FCS placement. Hence, the optimal position of FCSs in this case has the least power losses when compared with others. The power losses obtained from **CS1** to **CS6** are continually increasing as a result of the increasing power losses in the objective function. Table 4 presents the results obtained for the locations of the FCSs having real power losses, reactive power losses and cost function values in all examined cases. Furthermore, in all proposed cases, the real and reactive power flow in the lines of the EDN distribution network are obtained. Also, real and reactive power flow decline from **CS1** to **CS6** as shown in Fig. 4. However, the normalized value of investment cost increases from **CS1** to **CS6** as shown in Table 4 for the placement of FCSs. Conversely, the investment cost decreases in the placement of FCSs with SDGs as depicted in Table 5.

5.2.3. Results of voltage profile

The voltage at respective buses is shown in Figs. 6 to 11 for all cases suggested in this research. Fig. 6 depicts the voltage of the EDN network's buses for the FCS placements and FCS placement with SDG in **CS1**. The result shows that in **CS1**, the FCS's deployment decreases, while it increase in the FCSs placement with SDG positions. Similarly, the voltages in **CS2** during FCS placement and FCS placement with SDG are shown in Fig. 7. Furthermore, in the installation of FCSs with SDGs, the voltages in **CS3** are improved, as seen in Fig. 8. It is observed that voltages in the deployment of FCS with SDG is equivalent to the base case illustrated in Fig. 9. Finally, the voltages of the FCS placement with RES are stronger than the base case in **CS5** and **CS6**, as shown in Figs. 10, and 11 and also performance of all suggested algorithm are illustrated in Fig. 12.

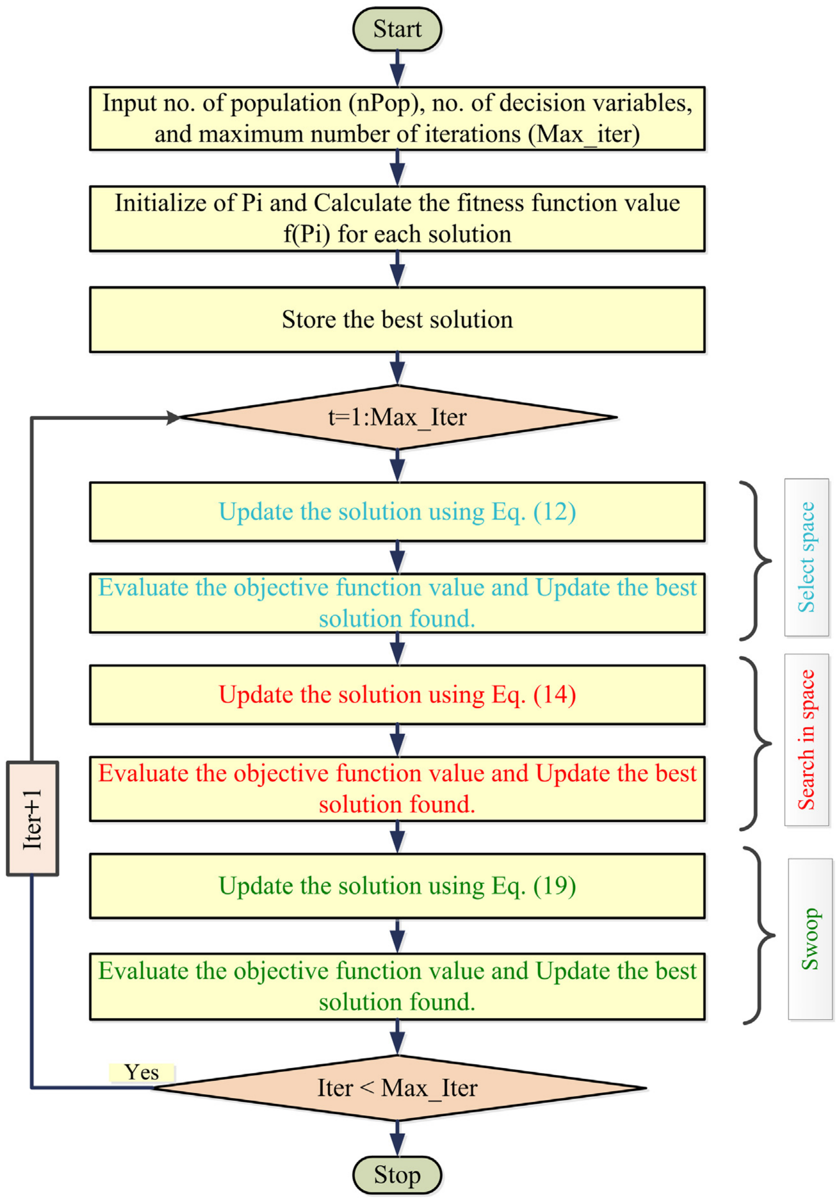

Fig. 3. Flowchart of the Improved bald eagle search algorithm (Ramadan et al., 2021).

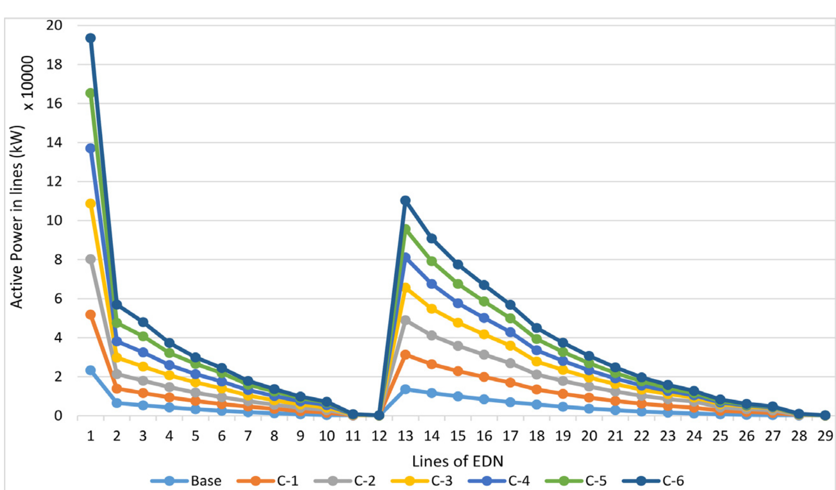

Fig. 4. Active power flow with FCS placement.

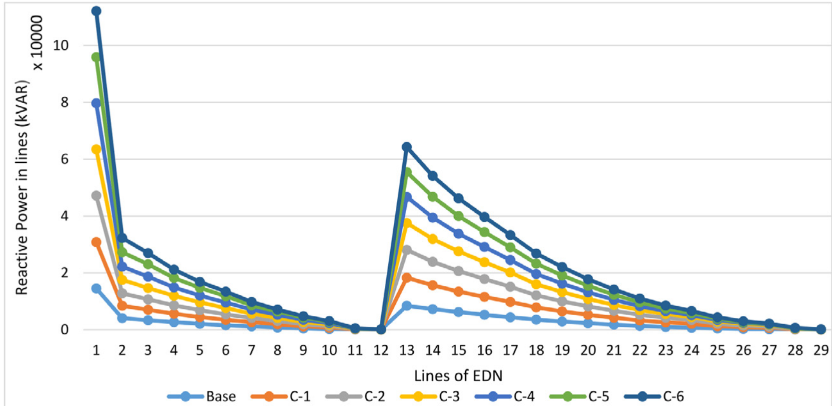

Fig. 5. Reactive power flow with FCS placement.

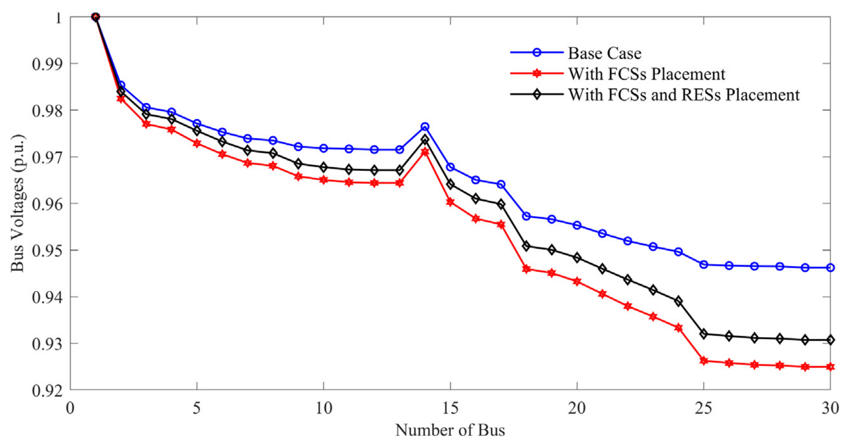

Fig. 6. Voltage of the buses for **CS1**.

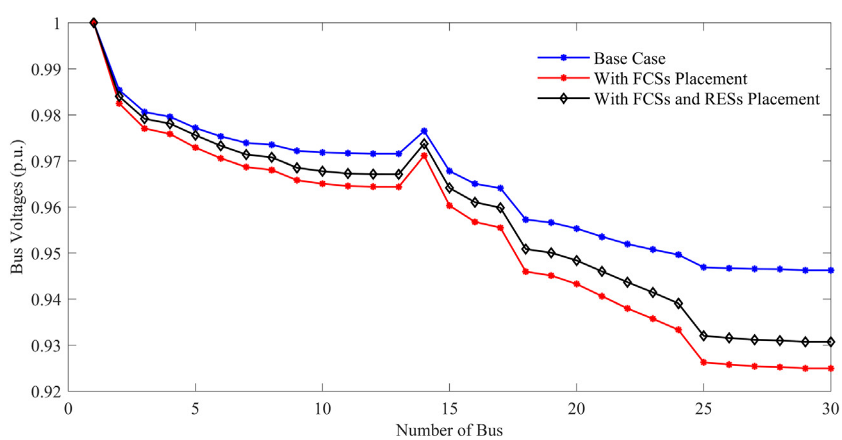

Fig. 7. Voltage of the buses for **CS2**.

Table 4
Results with FCSs placement.

Cases	w_1	w_2	w_3	Ploss (kW)	Qloss (kVAR)	Norm. IC	Cost Fun.	Optimal locations
Base	–	–	–	807.63	362.13	–	–	–
CS1	0	0	1	1277.73	562.46	0.4735	0.4735	11,14,18,25,28
CS2	0.1	0.1	0.8	1277.73	562.46	0.4735	0.4512	11,14,18,25,28
CS3	0.2	0.2	0.6	1193.69	531.43	0.4887	0.4216	7,11,14,18,28
CS4	0.3	0.3	0.4	1054.71	480.11	0.5586	0.3754	2,4,11,14,15
CS5	0.4	0.4	0.2	1047.95	477.61	0.5761	0.3036	2,4,7,11,14
CS6	0.5	0.5	0.0	1014.48	465.25	0.7200	0.2127	2,3,4,5,14

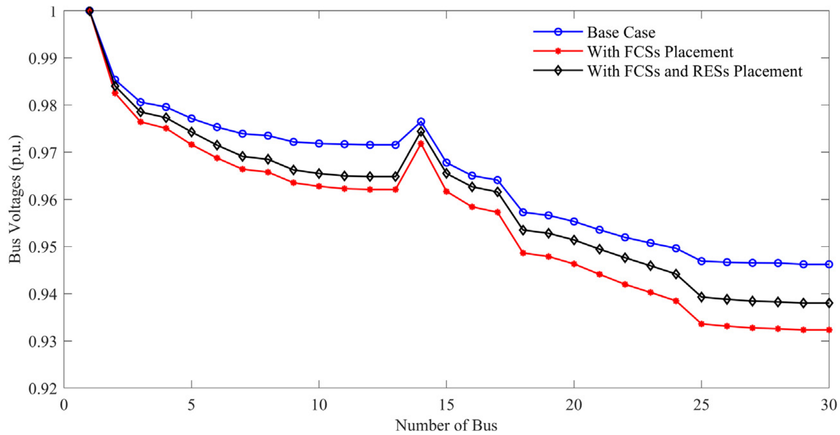

Fig. 8. Voltage of the buses for **CS3**.

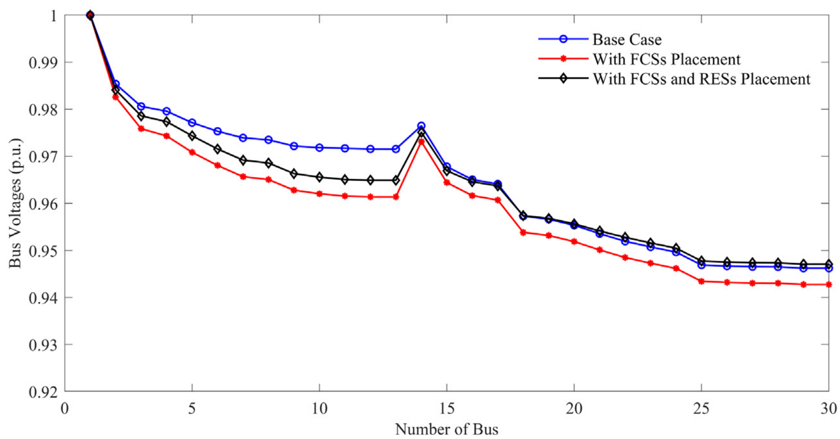

Fig. 9. Voltage of the buses for **CS4**.

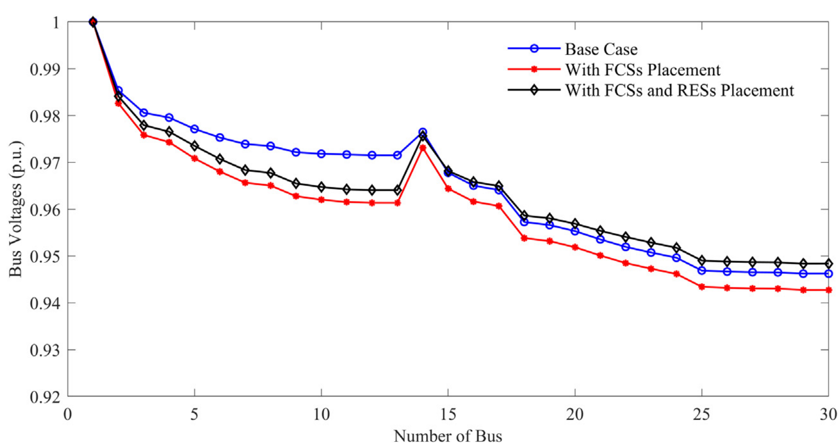

Fig. 10. Voltage of the buses for **CS5**.

Table 5
Results with FCSs and SDGs placement.

Cases	w_1	w_2	w_3	Ploss (kW)	Qloss (kVAR)	Norm. IC	Cost Fun.	Optimal locations
Base	–	–	–	550.46	247.90	–	–	–
CS1	0	0	1	1067.23	469.83	0.4735	0.4735	11,14,18,25,28
CS2	0.1	0.1	0.8	1067.23	469.83	0.4735	0.4745	11,14,18,25,28
CS3	0.2	0.2	0.6	991.13	441.77	0.4887	0.4699	7,11,14,18,28
CS4	0.3	0.3	0.4	881.09	401.20	0.5337	0.4487	2,7,11,14,15
CS5	0.4	0.4	0.2	861.59	394.01	0.5761	0.4079	2,4,7,11,14
CS6	0.5	0.5	0	829.68	382.24	0.7200	0.3440	2,3,4,5,14

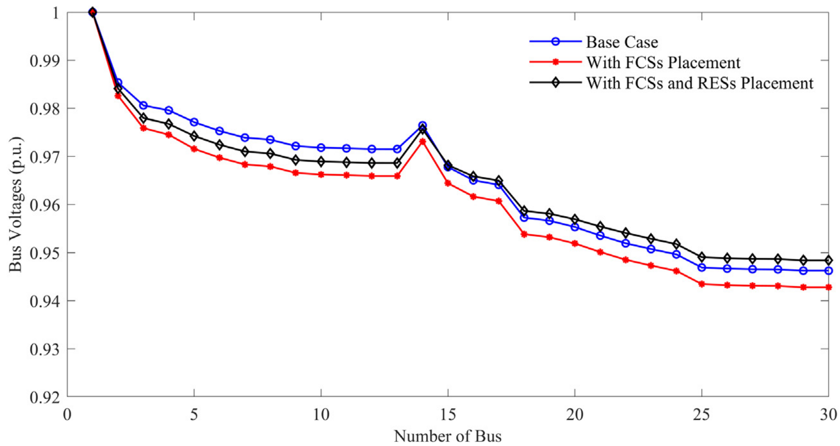

Fig. 11. Voltage of the buses for **CS6**.

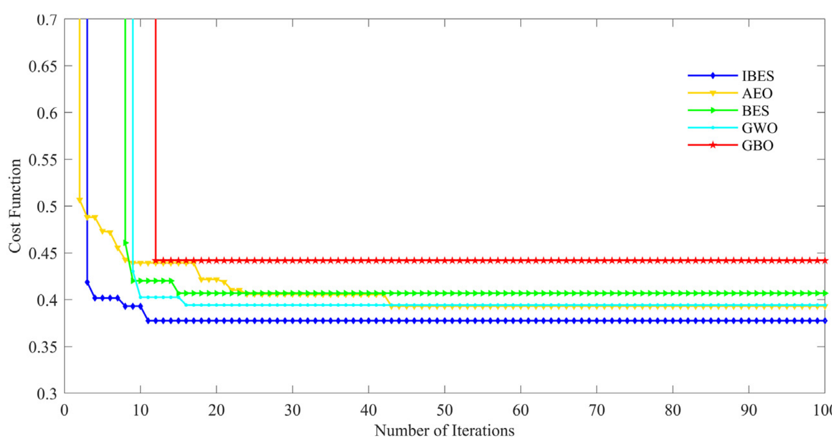

Fig. 12. Performance analysis of suggested algorithm.

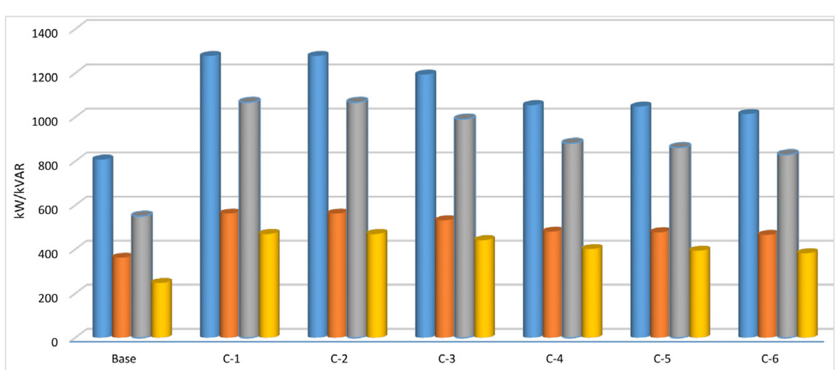

Fig. 13. Total active power and reactive power losses.

5.2.4. Results of power losses

For the placement of FCSs in the proposed EDN network, the real power loss is declined by 20.6% in **CS6** over **CS1**, the reactive power loss reduced by 17.28% in **CS6** against **CS1**, and the investment cost dropped by 34.23% in **CS1** against **CS6**. Fig. 13 depicts the real and reactive power loss in deploying FCSs without SDGs integration and the FCSs with SDGs integration. Furthermore, in the placement of FCSs with SDGs in the proposed EDN network, the power loss dropped by 22.23% for **CS6** over **CS1**, the reactive power loss reduced by 18.64% for **CS6** over **CS1**, and the investment costs declined by 34.23% for **CS1** over **CS6**. Figs. 14 and 15 illustrate the active and reactive power flow with the adoption of FCS with the installation of SDGs, respectively.

5.3. Reliability analysis for the east delta network

The main objective and purpose are to address a comprehensive evaluation of the impact of FCS and PVDG placement

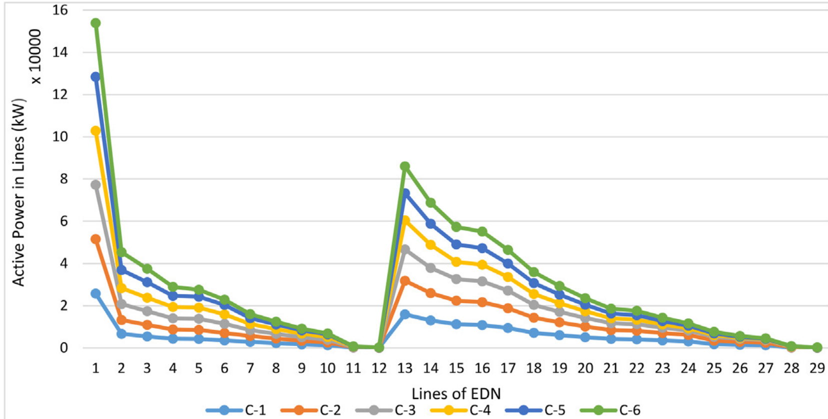

Fig. 14. Active power flow with FCS and RES placement.

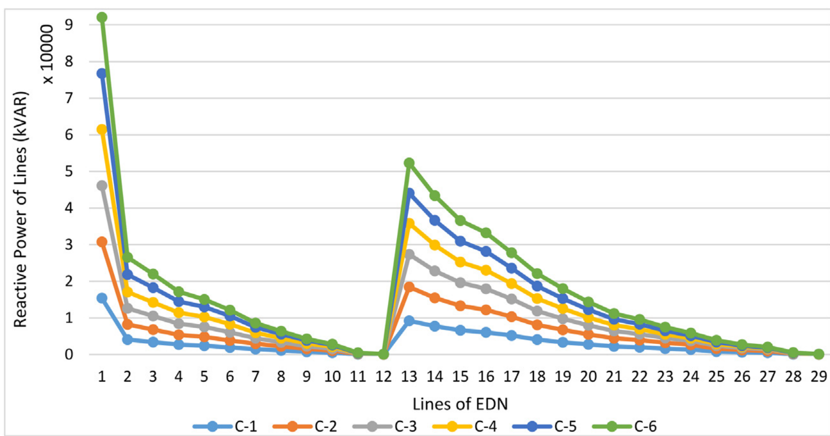

Fig. 15. Reactive power flow with FCS and SDGs placement.

Table 6
Reliability indices for the placement of FCSs.

Case	SAIFI	SAIDI	CAIDI	EENS	AENS
Base	0.1008	0.4785	4.7474	4719.65	5.69319
CS1	0.1768	0.9189	5.1981	13 228.92	15.9576
CS2	0.1768	0.9189	5.1981	13 228.92	15.9576
CS3	0.1162	0.5753	4.9505	10 220.32	12.3285
CS4	0.1062	0.4946	4.6593	8569.31	10.3369
CS5	0.1139	0.5459	4.7949	8160.87	9.84423
CS6	0.1054	0.487	4.6189	5730.17	6.91215

Table 7
Reliability indices for the placement of FCSs with SDGs.

Case	SAIFI	SAIDI	CAIDI	EENS	AENS
Base	0.10081	0.4785	4.7474	4719.65	5.69319
CS1	0.17494	0.9113	5.2093	12 799.4	15.4395
CS2	0.17494	0.9113	5.2093	12 799.4	15.4395
CS3	0.11437	0.5677	4.9637	9790.80	11.8103
CS4	0.10431	0.4869	4.6686	8139.79	9.81880
CS5	0.11200	0.5382	4.8058	7731.35	9.32610
CS6	0.10358	0.4793	4.6275	5265.14	6.35110

on the reliability of the EDN bus system. After deploying FCS and SDGs, reliability indices are computed for all of the case studies mentioned above. The base value of SAIFI is 0.10081 failure/customers and after the placement of FCSs, SAIFI value increased for different configurations as expressed in Table 6. Similarly, the other reliability indices are also increased after the integration of EV load at the distribution system.

All the reliability indices as mentioned above for all the case studies are depicted in Fig. 16 integration of EV load, the distribution system's reliability has been analyzed with the placement of FCS and SDGs. The value of SAIFI, SAIDI, CAIDI, EENS and AENS have been compared for the proposed six case studies. The value of reliability indices is improved compared with the first case in which only FCS has been considered. Therefore, the reliability of the distribution system is improved when the placement of FCS and SDGs are considered as given in Table 7. from the analysis of the reliability of the distribution system for different case studies as mentioned above, and the reliability has better when EV load placed near to the grid, the value of reliability indices for different case studies are shown in Fig. 17.

6. Conclusion and recommendations

The article presents an optimal deployment model of the fast EV charging station and the integration of renewable energy sources. It suggests a novel approach for deploying the fast-charging station with minimum investment and power loss in the distribution system while maintaining voltage stability and

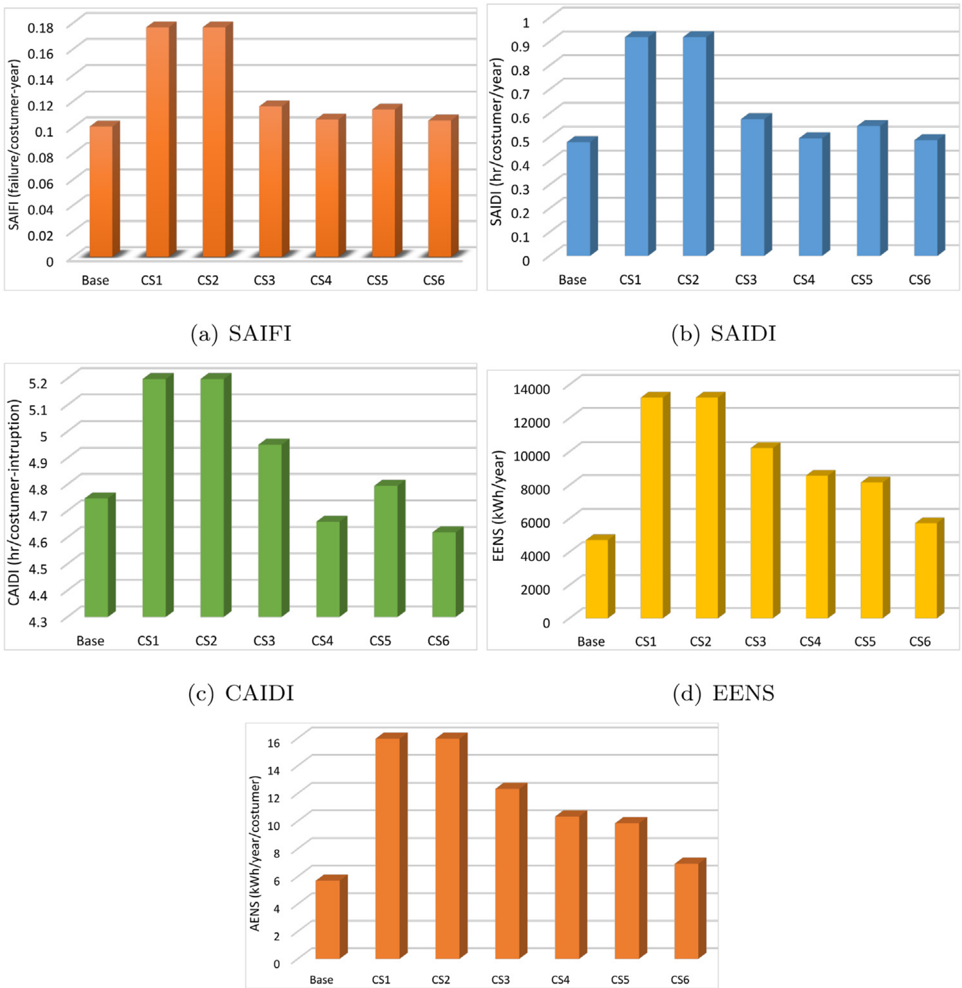

(a) SAIFI

(b) SAIDI

(c) CAIDI

(d) EENS

(e) AENS

Fig. 16. Reliability indices for integration of FCSs.

power quality. An improved version of the bald eagle search algorithm is presented for placing FCSs with randomly placed solar-based distribution generation in the EDN system. The derived benchmark functions demonstrate the superiority of the suggested algorithm. Moreover, six case studies are presented for installing the FCSs based on active and reactive power loss with investment costs for installing the charging station. Furthermore, the distribution system's reliability has been analyzed for the placement of FCSs and FCSs with SDG integration in the distribution network.

The authors expect this work to support the grid integration of EVs, reduce carbon emissions, and inspire investors to install the FCSs. Furthermore, additional studies and innovations are needed to place charging stations. Hence, future work may include various power management strategies incorporating EVs into the grid and vehicle-to-home features of the CS to improve the distribution network's performance.

CRediT authorship contribution statement

Fareed Ahmad: Conceptualization, Methodology/Study design, Software, Validation, Formal analysis, Resources, Writing – original draf, Writing – review and editing. **Imtiaz Ashraf:** Investigation, Visualization, Supervision, Project administration. **Atif Iqbal:** Investigation, Visualization, Supervision, Funding acquisition. **Mousa Marzband:** Investigation, Supervision. **Irfan Khan:** Investigation, Supervision.

Declaration of competing interest

The authors declare that they have no known competing financial interests or personal relationships that could have appeared to influence the work reported in this paper.

Data availability

The data that has been used is confidential.

Acknowledgments

This publication was made possible by NPRP grant # [NPRP-13S-0108-20008] from the Qatar National Research Fund (a member of Qatar Foundation). The statements made herein are solely the responsibility of the authors. The APC is funded by Qatar National Library, Doha, Qatar.

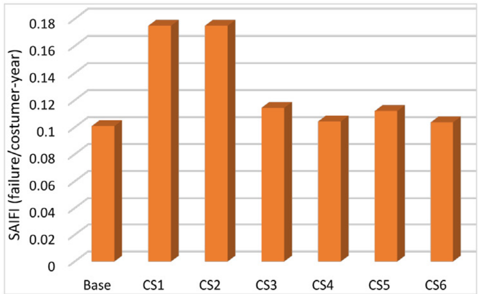

(a) SAIFI

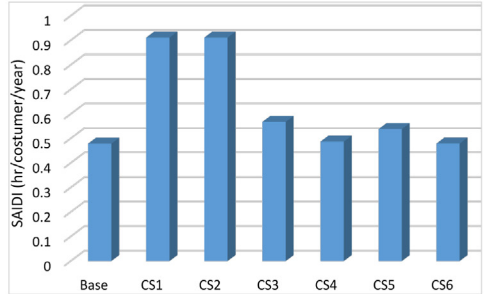

(b) SAIDI

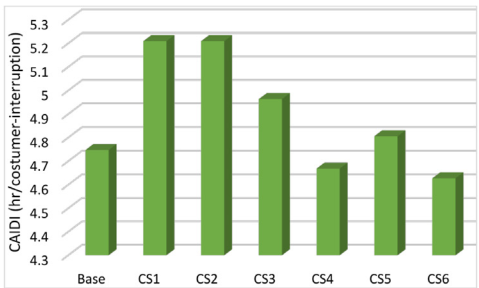

(c) CAIDI

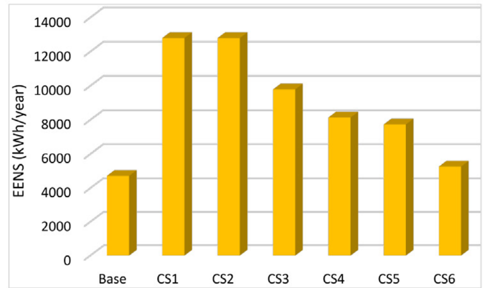

(d) EENS

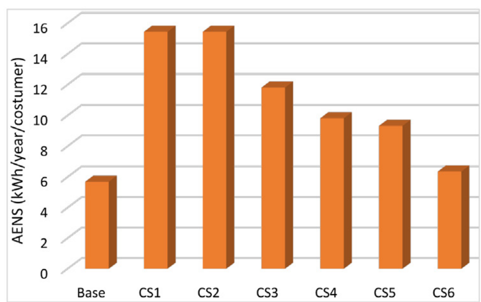

(e) AENS

Fig. 17. Reliability indices for integration of FCSs with SDGs.

References

Ahmad, F., Iqbal, A., Ashraf, I., Marzband, M., Khan, I., 2022a. Placement of electric vehicle fast charging stations in distribution network considering power loss, land cost, and electric vehicle population. Energy Sources A: Recovery Util. Environ. Eff..

Ahmad, F., Iqbal, A., Ashraf, I., Marzband, M., Khan, I., 2022b. Placement of electric vehicle fast charging stations using grey wolf optimization in electrical distribution network. In: 2022 IEEE International Conference on Power Electronics, Smart Grid, and Renewable Energy (PESGRE). pp. 1–6.

Ahmad, F., Iqbal, A., Ashraf, I., Marzband, M., et al., 2022c. Optimal location of electric vehicle charging station and its impact on distribution network: A review. Energy Rep. 8, 2314–2333.

Ahmed, A., Iqbal, A., Khan, I., Al-Wahedi, A., Mehrjerdi, H., Rahman, S., 2021. Impact of EV charging station penetration on harmonic distortion level in utility distribution network: A case study of Qatar. In: 2021 IEEE Texas Power and Energy Conference (TPEC). pp. 1–6.

Alsattar, H., Zaidan, A., Zaidan, B., 2020. Novel meta-heuristic bald eagle search optimisation algorithm. Artif. Intell. Rev. 53 (3), 2237–2264.

Archana, A., Rajeev, T., 2021. A novel reliability index based approach for EV charging station allocation in distribution system. IEEE Trans. Ind. Appl. 57 (6), 6385–6394.

Battapothula, G., Yammani, C., Maheswarapu, S., 2019. Multi-objective optimal planning of FCSs and DGs in distribution system with future EV load enhancement. IET Electr. Syst. Transp. 9 (3), 128–139.

Bilal, M., Rizwan, M., 2021. Integration of electric vehicle charging stations and capacitors in distribution systems with vehicle-to-grid facility. Energy Sources A: Recovery Util. Environ. Eff. 1–30.

Bilal, M., Rizwan, M., Alsaidan, I., Almasoudi, F.M., 2021. AI-based approach for optimal placement of EVCS and DG with reliability analysis. IEEE Access 9, 154204–154224.

Bitencourt, L., Abud, T.P., Dias, B.H., Borba, B.S., Maciel, R.S., Quirós-Tortós, J., 2021. Optimal location of EV charging stations in a neighborhood considering a multi-objective approach. Electr. Power Syst. Res. 199, 107391.

Chen, L., Xu, C., Song, H., Jermsittiparsert, K., 2021. Optimal sizing and sitting of EVCS in the distribution system using metaheuristics: A case study. Energy Rep. 7, 208–217.

Cheng, J., Xu, J., Chen, W., Song, B., 2022. Locating and sizing method of electric vehicle charging station based on improved whale optimization algorithm. Energy Rep. 8, 4386–4400.

Deb, S., Tammi, K., Kalita, K., Mahanta, P., 2018. Impact of electric vehicle charging station load on distribution network. Energies 11 (1), 1–25.

El-Ela, A.A.A., El-Sehiemy, R.A., Kinawy, A.-M., Mouwafi, M.T., 2016. Optimal capacitor placement in distribution systems for power loss reduction and voltage profile improvement. IET Gener. Transm. Distrib. 10 (5), 1209–1221.

Electrek, 2021. URL https://electrek.co/2021/11/09/thenumberofuselectricvehiclesgrowsfrom16kto2millionin-10years/.

Faddel, S., Al-Awami, A.T., Mohammed, O.A., 2018. Charge control and operation of electric vehicles in power grids: a review. Energies 11 (4).

Gandoman, F.H., Ahmadi, A., Van den Bossche, P., Van Mierlo, J., Omar, N., Nezhad, A.E., Mavalizadeh, H., Mayet, C., 2019. Status and future perspectives of reliability assessment for electric vehicles. Reliab. Eng. Syst. Saf. 183, 1–16.

Gielen, D., Boshell, F., Saygin, D., Bazilian, M.D., Wagner, N., Gorini, R., 2019. The role of renewable energy in the global energy transformation. Energy Strategy Rev. 24, 38–50.

Li, C., Zhang, L., Ou, Z., Wang, Q., Zhou, D., Ma, J., 2022. Robust model of electric vehicle charging station location considering renewable energy and storage equipment. Energy 238, 121713.

Lotfi, M., Monteiro, C., Javadi, M.S., Shafie-khah, M., Catalão, J.P., 2019. Optimal prosumer scheduling in transactive energy networks based on energy value signals. In: 2019 International Conference on Smart Energy Systems and Technologies (SEST). pp. 1–6.
Luo, C., Huang, Y.F., Gupta, V., 2017. Placement of EV charging stations-balancing benefits among multiple entities. IEEE Trans. Smart Grid 8 (2), 759–768.
Luo, X., Qiu, R., 2020. Electric vehicle charging station location towards sustainable cities. Int. J. Environ. Res. Public Health 17 (8).
Luo, L., Wu, Z., Gu, W., Huang, H., Gao, S., Han, J., 2020. Coordinated allocation of distributed generation resources and electric vehicle charging stations in distribution systems with vehicle-to-grid interaction. Energy 192, 116631.
Mainul Islam, M., Shareef, H., Mohamed, A., 2018. Optimal location and sizing of fast charging stations for electric vehicles by incorporating traffic and power networks. IET Intell. Transp. Syst. 12 (8), 947–957.
Michaelides, E.E., 2021. Primary energy use and environmental effects of electric vehicles. World Electr. Veh. J. 12 (3), 138.
Mohsenzadeh, A., Pazouki, S., Ardalan, S., Haghifam, M.R., 2018. Optimal placing and sizing of parking lots including different levels of charging stations in electric distribution networks. Int. J. Ambient Energy 39 (7), 743–750.
Moradi, M.H., Abedini, M., Tousi, S.M.R., Hosseinian, S.M., 2015. Electrical power and energy systems optimal siting and sizing of renewable energy sources and charging stations simultaneously based on differential evolution algorithm. Int. J. Electr. Power Energy Syst. 73, 1015–1024.
Nanaki, E.A., Koroneos, C.J., 2016. Climate change mitigation and deployment of electric vehicles in urban areas. Renew. Energy 99, 1153–1160.
Pal, A., Bhattacharya, A., Chakraborty, A.K., 2021. Allocation of electric vehicle charging station considering uncertainties. Sustain. Energy Grids Netw. 25, 100422.
Phonrattanasak, P., Leeprechanon, N., 2012. Optimal location of fast charging station on residential distribution grid. Int. J. Innov. Manage. Technol. 3 (6), 675.
Rajesh, P., Shajin, F.H., 2021. Optimal allocation of EV charging spots and capacitors in distribution network improving voltage and power loss by quantum-behaved and Gaussian mutational dragonfly algorithm (QGDA). Electr. Power Syst. Res. 194, 107049.
Ramadan, A., Kamel, S., Hassan, M.H., Khurshaid, T., Rahmann, C., 2021. An improved bald eagle search algorithm for parameter estimation of different photovoltaic models. Processes 9 (7), 1127.
Reddy, M.S.K., Selvajyothi, K., 2020. Optimal placement of electric vehicle charging station for unbalanced radial distribution systems. Energy Sources A: Recovery Util. Environ. Eff. 00 (00), 1–15.
Reports, V., 2020. URL https://www.prnewswire.com/newsreleases/distributedgenerationmarketsizeisprojectedtoreachusd118,898.35millionby2025-valuatesreports301133254.html.
Sambaiah, K.S., Jayabarathi, T., 2021. Optimal reconfiguration and renewable distributed generation allocation in electric distribution systems. Int. J. Ambient Energy 42 (9), 1018–1031.
Tavakoli, A., Saha, S., Arif, M.T., Haque, M.E., Mendis, N., Oo, A.M., 2020. Impacts of grid integration of solar PV and electric vehicle on grid stability, power quality and energy economics: a review. IET Energy Syst. Integr. 2 (3), 243–260.